A Platinum Open Access Journal for Organic Chemistry

Paper

Free to Authors and Readers | DOAJ Seal | *Arkivoc* **2022**, part iii, 327-338

A comparative study of biradicaloids as ligands in iron tetracarbonyl complexes

M. T. Scharnhölz,[a] P. Coburger,*[a] H. Beer,[b] J. Bresien,[b] A. Schulz,[b,c] and H. Grützmacher[a]

[a] *Department of Chemistry and Applied Biosciences, ETH Zürich Vladimir-Prelog-Weg 1, 8093 Zürich, Switzerland*

[b] *Institut für Chemie, Universität Rostock Albert-Einstein-Str. 3a, 18059 Rostock, Germany*

[c] *Leibniz-Institut für Katalyse an der Universität Rostock e.V. (LIKAT) Albert-Einstein-Str. 29a, 18059 Rostock, Germany*

Email: pcoburger@inorg.chem.ethz.ch hgruetzmacher@ethz.ch

Received 09-02-2022 **Accepted Manuscript** 11-30-2022 **Published on line** 12-15-2022

Abstract

Iron tetracarbonyl complexes of the biradicaloids [P(μ-N-Ter)]$_2$ (Ter: 2,6-dimesitylphenyl) and [P(μ-C-IPr)]$_2$ (IPr: 1,3-bis(2,6-di*iso*propylphenyl)imidazol-2-ylidene) have been isolated. These two biradicaloids act here as σ-donating, monodentate ligands. Experimental and theoretical data suggest that they can best be described in their zwitterionic resonance structures in these complexes. Single-crystal XRD and IR spectroscopy reveal that the donor strength of both is comparable to *N*-heterocyclic carbenes (NHCs). [P(μ-C-IPr)]$_2$ is a slightly stronger donor than [P(μ-N-Ter)]$_2$. Furthermore, an improved, scalable, and facile synthesis of both biradicaloids is presented.

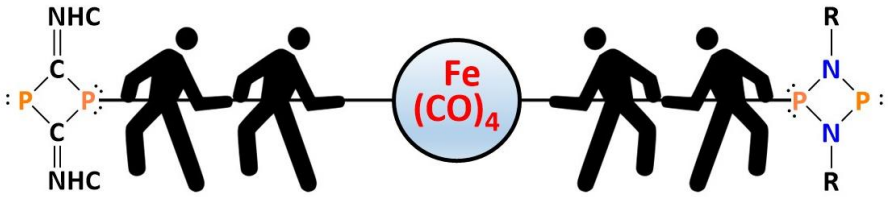

Keywords: Biradicaloids, coordination chemistry, iron complexes, *N*-heterocyclic carbenes

 ©AUTHOR(S)

Introduction

Four-membered biradicaloids have gained significant attention over the last two decades.[1] While biradicals based on carbon skeletons are elusive and highly reactive species, incorporation of main-group elements increases their stability and decreases their biradical character.[2] These derivatives are often referred to as "biradicaloids".[3, 4] A milestone has been the isolation of 1,3-diphospha-cyclobutane-2,4-diyl by Niecke.[5] It is the first example of a stable biradicaloid that can be isolated in gram scale.[6]

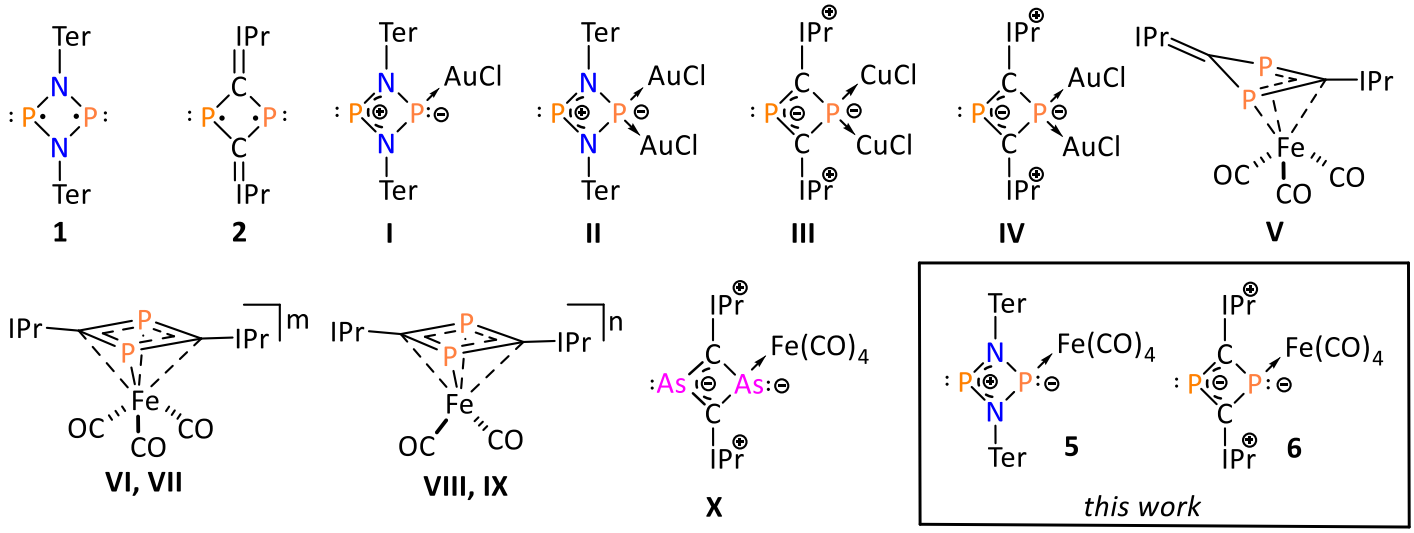

Scheme 1. Transition-metal complexes of the biradicaloids [P(μ-NTer)]$_2$ (**1**) and [P(μ-CIPr)]$_2$ (**2**). Coinage metal complexes of **1** (**I**, **II**) and **2** (**III** and **IV**)[1, 7] ; iron complexes of **2**: **VI**: m = +1, **VII**: m = +2; **VIII**: n = +1, **IX**: n = 0. Partial charges in **V** – **IX** were omitted for clarity.[8] Fe(CO)$_4$ complex of the biradicaloid [As(μ-C-IPr)]$_2$ (**X**).[9]

Further examples of biradicaloids were presented by Bertrand,[10] Power,[11] Schulz (**1**),[12] Grützmacher (**2**)[13] and others.[6] Reactivities of **1** and **2** towards small molecules,[13, 14] alkenes,[14] alkines,[1] oxidizing agents[13, 15] Lewis acids[7] and Lewis bases[7] were studied in detail. In these studies, it was shown that these species with a central 6π-electron system may react in the fashion of radicals, zwitterions or aromatic compounds. The combination of high reactivity and the presence of several potential donor atoms in **1** and **2** also make them intriguing ligands for transition metals. Indeed, it was found that **2** can act as a remarkable π-donating ligand (compare Scheme 1).[16] Especially interesting is a series of Fe(CO)$_3$ (**V**, **VI** and **VII**) and Fe(CO)$_2$ (**VIII** and **IX**) complexes, which show a rich-redox chemistry. It was also shown that **2** can act as a redox non-innocent ligand and may change its hapticity from η^3 to η^4.[8]

In contrast, the coordination chemistry of **1** is rather underexplored and is limited to gold chloride complexes **I** and **II**.[7] Similar copper (**III**) and gold (**IV**) complexes are also known for **2**.[1] Only recently, an Fe(CO)$_4$ complex of the biradicaloid [As(μ-C-IPr)]$_2$ (**X**) was published by the Ghadwal group.[9]

Considering these findings, the further investigation of the coordination chemistry of biradicaloids **1** and **2** towards iron carbonyl fragments seemed worthwhile. The coordination of Fe(CO)$_4$ fragments is especially interesting since they are expected to bind to the phosphorus atoms in **1** and **2** in a mono-dentate fashion. To the best of our knowledge, no study has been published so far which directly compares the properties of the two biradicaloids in the same reaction or compound. This would yield additional insight into the σ-donating

 ©AUTHOR(S)

properties of the biradicaloids by comparison of the frequencies of the CO-stretching vibrations. In this paper, the results of these experimental efforts are reported.

Results and Discussion

The synthesis of **1** has been improved multiple times.[17] Here, an upscaled procedure is given that makes it accessible on a multi-gram scale [see the experimental section] (yield for the reduction: 62%, overall yield starting from Ter−NH_2: 47%). The original synthetic procedure for the synthesis of **2**, in which an N-heterocyclic phosphane was used to scavenge an oxygen atom from sodium 2-phospha-ethynolate [Na(OCP)] under reductive conditions, is laborious. It is lengthy and does not scale to more than 150 mg of product.[13] An improved procedure was published, which allows the synthesis of **2** on a larger scale, however, two very time consuming steps are still involved.[18] In light of the increased number of interesting coordination compounds of **2**, a facile synthesis is required to allow for a convenient exploration of their follow-up chemistry.

The protocol described here - in contrast to the original procedure - utilizes commercial Ph_3SiCl to scavenge oxygen from Na(OCP). It had been reported already that Na(OCP) reacts with chloro(triphenyl)silane to form **3**, and that **3** could then rearrange in the presence of the NHC-carbon atoms which initiate the rearrangement upon which the carbene becomes a substituent in the molecule to **4** (see Scheme 2).[19]

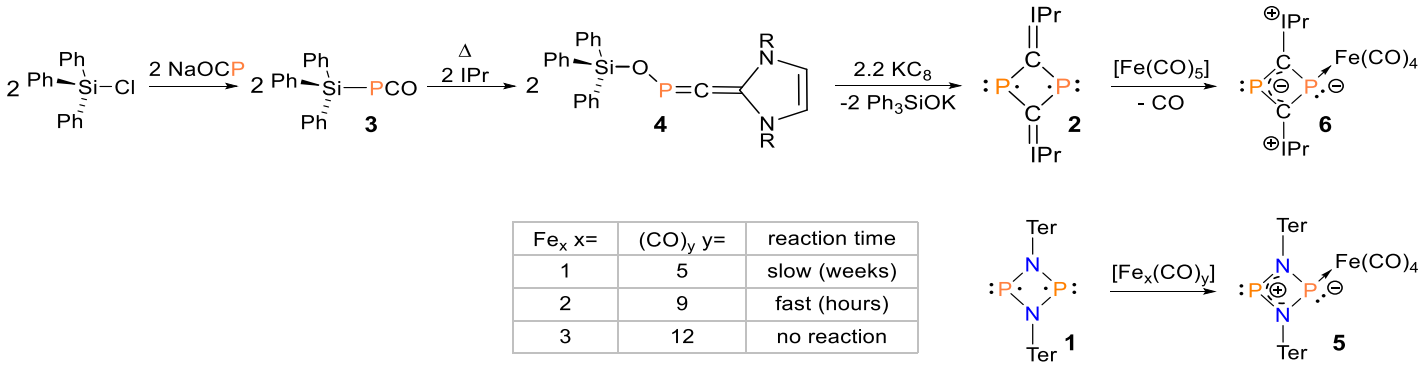

Fe_x x=	$(CO)_y$ y=	reaction time
1	5	slow (weeks)
2	9	fast (hours)
3	12	no reaction

Scheme 2. Top row: New reaction sequence for the synthesis of **2** and reaction with $[Fe(CO)_5]$ to form **6**. Bottom row: reaction of **1** with iron carbonyls ($[Fe(CO)_5]$, $[Fe_2(CO)_9]$, $[Fe_3(CO)_{12}]$) and the reaction times for quantitative formation of **5**. For both biradicaloids the leading resonance structure is depicted.

Reduction of **4** also resulted in the formation of **2**. The selectivity in the formation of **4** could be enhanced by using toluene with only small amounts of tetrahydrofuran (THF) as solvents at 80 °C. Subsequently, the reduction with KC_8 was best carried out in *n*-hexane at low temperature (−78 °C). Extraction of the crude product with diethyl ether gave a clean product without recrystallization (for details see experimental section). Under these reaction conditions, compound **2** is accessible in a one-step, one-pot reaction, and the product was obtained in 35% yield (calculated relative to IPr) on multi-gram scale. Furthermore, it avoids any olfactory irritation arising from the phosphino phosphaketene which is a reaction step in the old protocol.

To prepare a tetracarbonyl complex, **1** was treated with $[Fe(CO)_5]$ in toluene. The reaction proceeded very slowly (33% conversion after 7 days as monitored by $^{31}P\{^1H\}$ NMR spectroscopy). The product showed doublet-of-doublets resonances at δ: 275.3 ppm and 357.1 ppm; $^2J(^{31}P, ^{31}P)$ 174 Hz), indicating that the two

 ©AUTHOR(S)

phosphorus ring atoms became inequivalent in the reaction with pentacarbonyl iron(0). Using one equivalent of $[Fe_2(CO)_9]$ as the source of the $Fe(CO)_4$ moiety gave full conversion after 16 h reaction time at room temperature. $Fe(CO)_5$ Was acting as a leaving group in this reaction. No reaction could be observed between $[Fe_3(CO)_{12}]$ and **1** (cf. Scheme 2).

When **2** was reacted with pentacarbonyl iron(0) at 130 °C, the tricarbonyl complex **V** was obtained.[8] When the reaction was carried out at room temperature in toluene, the tetra-carbonyl complex (**6**, Scheme 2) was obtained. Within minutes, the color changed from moss green to dark purple via brownish red. An iron(tetracarbonyl) fragment coordinates to **2** *via* one phosphorus atom (as shown by X-ray crystallography, *vide infra*), and CO was liberated. The $^{31}P\{^1H\}$ NMR spectrum of the reaction mixture showed a pair of doublet resonances at δ: 79.8 and 325.7 ppm [$^2J(^{31}P, ^{31}P)$ 119 Hz].

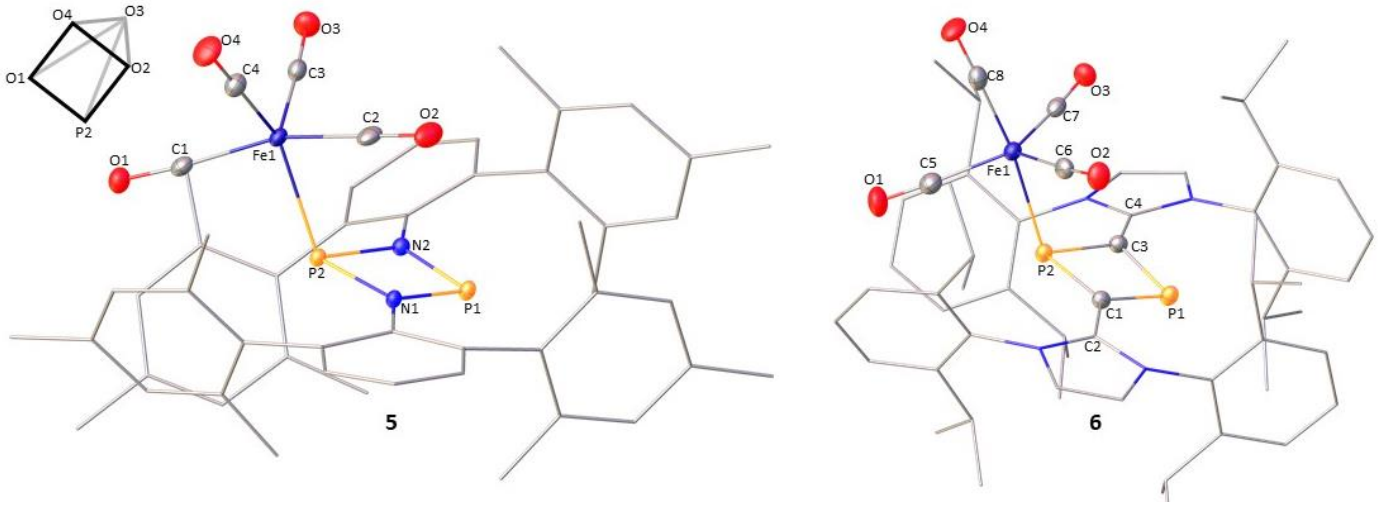

Figure 1. Solid-state structures of **5** and **6**. Protons and solvents are omitted for clarity. Color code: carbon (grey), nitrogen (blue), phosphorus (orange), iron (dark blue), oxygen (red). Selected distances [Å]: **5**: N1−P1 1.681(1), N2−P1 1.664(1), N1−P2 1.797(1), N2−P2 1.775(1), P2−Fe1 2.2657(4), O1−C1 1.147(2), O2−C2 1.148(2), O3−C3 1.147(2), O4−C4 1.149(2); **6**: C1−C2 1.398(3), C3−C4 1.409(3), C1−P1 1.764(3), C3−P1 1.745(2), C1−P2 1.824(2), C3−P2 1.820(2), P2−Fe1 2.3648(7), O1−C5 1.143(3), O2−C6 1.159(3), O3−C7 1.158(3), O4−C8 1.149(3).

The structure of **5** [determined by X-ray diffraction methods (XRD)] shows evidence for the zwitterionic polarization of the radical electrons in the central ring (see Figure 1), which is in agreement with the NMR data discussed above. Distances from the coordinated P-atom to the nitrogen atoms in the ring are elongated in comparison to the starting material (Ø=1.786(1) Å vs. 1.717(1) Å[12]) while distances of the non-coordinated P-atom are shortened compared to the starting material (Ø=1.673(1) Å vs. 1.717(1) Å[12]). The P2-Fe1 bond towards the iron carbonyl moiety is bent out of the central N_2P_2 plane by 60°. The environment around the iron center can best be described as a distorted square pyramidal with ligand **1** in one of the basal positions, which is reflected by the structural parameter τ_5[20] of 0.32 for **5** (see also Table S5, SM). In **6**, the central four-membered C_2P_2 ring may be described in the same zwitterionic manner as above. The two distances from the coordinated phosphorus atom to the ring carbon atoms are elongated in comparison to the starting material (Ø=1.822 vs. 1.794 Å),[13] while the distance from the non-coordinated P-atom to the ring-C-atoms are shortened (Ø=1.755 vs. 1.794 Å).[13] The distances from the NHC-carbon atoms to the ring carbon atoms are slightly greater in comparison to the starting material (Ø=1.406 vs. 1.387Å),[13] which is an indicator of

 ©**AUTHOR(S)**

imidazolium character (a positive partial charge) of the NHC substituents.[8] The P-Fe bond here is bent out of the C_2P_2 plane by 57°, which is slightly less than in **5**. The P–$Fe(CO)_4$ moiety has a trigonal-bipyramidal shape at a structural parameter τ_5[20] of 0.76 (see also Table S5, SM).

The average C-O distances are shorter in **5** (Ø=1.148 Å) compared to **6** (Ø = 1.155 Å). The homologous C_2As_2 complex **X** has the same average CO bond distance as **6**.[9] This indicates that **1** acts as a weaker ligand than **2**, and that $IPr_2C_2As_2$ in **X** is similar in donor strength to **2**.[21] This claim is supported by CO stretching frequencies in the IR spectra, which are lower for **6** [**5**: 2034, 1967, 1949 cm^{-1} (overlap of two signals as indicated by calculations, see the SI, Figure S9 and S10), **6**: 2001, 1928, 1900, 1886 cm^{-1}]. Classical metal carbonyl fragments exhibit lower CO stretching frequencies when bearing stronger ligands.[22, 23] For both **5** and **6** this holds true. The observation of 4 CO stretching frequencies is in accordance with a C_1-symmetric coordination environment. CO-stretching frequencies of iron(tetracarbonyl) complexes were collected from literature for a series of compounds (Figure 2). It shows that nitrogen substitution on phosphorus leads to higher stretching frequencies than carbon substitution (compounds **A** and **B**, **C** and **D**). This trend aligns well with the data reported here. It also appears that biradicaloids **1** and **2** are stronger ligands in iron(tetracarbonyl) complexes than the other phosphane complexes **A** - **F** listed in Figure 2. The weaker donor $[P(\mu\text{-NTer})]_2$ (**1**) can be compared in donor strength to complexes with N-heterocyclic carbenes (NHCs) as ligands (see **G** – **K**) while phosphane while **2** is has a stronger electron-donating effect in comparison to all complexes displayed in Figure 2.

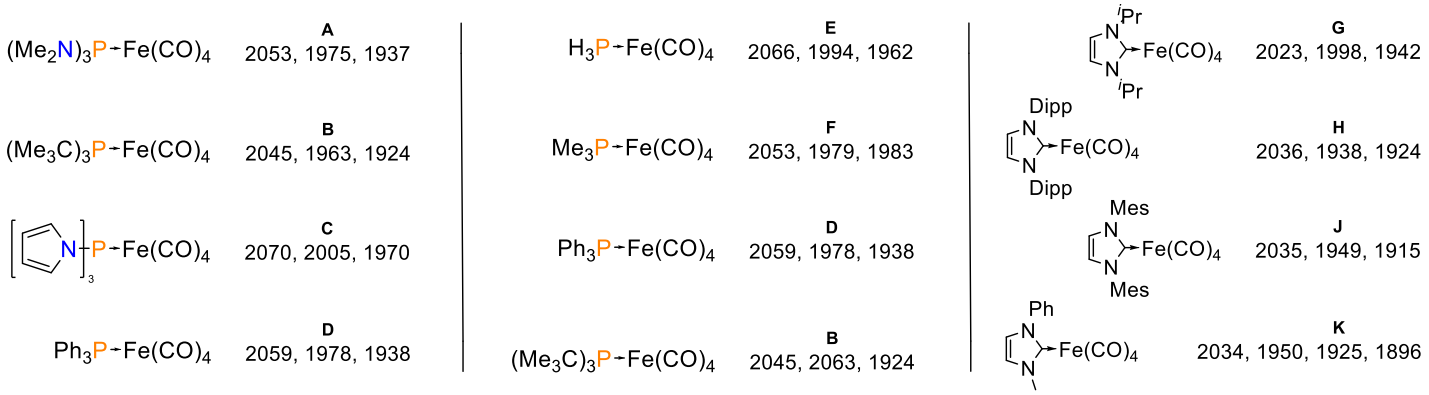

Figure 2. CO-stretching frequencies [cm^{-1}] of selected phosphane- and carbene iron(tetracarbonyl)-complexes. First column: comparison of carbon *vs*. nitrogen substitution; second column: increasing steric demand of phosphane substituent; third row: series of NHC complexes. Tris(dimethylamino)phosphane (**A**)[26], tris(*tert*-butyl)phosphane (**B**)[27], tris(*N*-pyrrolyl)phosphane (**C**)[28], tri(phenyl)phosphane (**D**)[29]; phosphane (**E**)[30], tri(methyl)phosphane (**F**)[28]; I^{i}Pr (1,3-bis(2,6-diisopropylphenyl)imidazolium-2-ylidene, (**G**)[31], IPr (1,3-bis(2,6-diisopropylphenyl)imidazol-2-ylidene, (**H**)[31], IMes (1,3-bis(2,4,6-trimethylphenyl)imidazol-2-ylidene, (**J**)[31], IPhMe (1-(phenyl)-3-(methyl)imidazol-2-ylidene, (**K**).[31]

It is known that the energy difference between a square-pyramidal and trigonal-bipyramidal coordination environment is small for d^8 complexes[24], which explains their highly dynamic behavior according to the Berry mechanism.[25] Thus, subtle steric and/or electronic effects may result in the preference of one of the coordination modes over the other. Therefore, calculations on derivatives bearing less steric bulk were carried out for the $Fe(CO)_4$ complexes **5** and **6** (**5'**: Ph instead of Ter; **6'**: H instead of Dipp, see the SM, chapter 2.2). Interestingly, both adopt a trigonal bipyramidal ligand environment. Thus, the different coordination

 ©**AUTHOR(S)**

environments in **5** and **6** in the solid state are likely caused by the different steric demand of the terphenyl and diisopropylphenyl groups in ligands **1** and **2**.

In addition, EDA-NOCV calculations[32, 33] (ORCA program package,[32] TPSS-D3BJ/def2-TZVP)[34, 35, 36, 37] were carried out to get a deeper insight into the Fe-L interactions in **5** and **6**. Both, **1** and **2** act as strong σ-donor and weak π-acceptor ligands in the tetracarbonyl complexes (see Figure S11 for a graphical representation). Thereby, in agreement with the conclusions drawn from IR-spectroscopy, **2** is a stronger σ-donor (68.3 vs. 50.6 kcal·mol^{-1}) and weaker π-acceptor (6.5 vs. 13.6 kcal·mol^{-1}) than **1**.

Conclusions

A scaled procedure has been provided for biradicaloid [P(μ-N-Ter)]$_2$, and a new and improved synthetic route was presented for biradicaloid. [P(μ-C-IPr)]$_2$. Their properties as ligands in the iron(tetracarbonyl) complexes were investigated and compared. It could be shown that both act as very strong σ-donor ligands to Fe(CO)$_4$ complex fragments, as revealed by IR spectroscopy and XRD experiments performed with single crystals. While the donor strength of [P(μ-N-Ter)]$_2$ is comparable to phosphanes such as PPh$_3$, the donor strength of [P(μ-C-IPr)]$_2$ exceeds the one of other phosphanes like PPh$_3$ and P*t*-Bu$_3$ and even *N*-heterocyclic carbenes.

Experimental Section

General. All air- and moisture-sensitive manipulations were carried out using standard vacuum line Schlenk techniques or in an MBraun inert atmosphere dry-box containing an atmosphere of purified argon. CD_2Cl_2 and C_6D_6 were purchased from Cambridge Isotope Laboratories. CD_2Cl_2 was dried over CaH_2 and distilled and C_6D_6 was distilled from sodium/benzophenone.

All glassware was either stored in a 130 °C oven for at least 16 hours and was degassed prior to use or flame dried. Solvents were degassed prior to the filtration over alumina in the PureSolv purification system and the water content was determined by Karl Fischer titration. DCM and acetonitrile were stored over molecular sieves (3 Å). For all other solvents, 4 Å molecular sieves were used.

1,3-Bis(2,6-di*iso*propylphenyl)-1,3-dihydro-2H-imidazol-2-ylidene (IPr) was synthesized from 1,3-bis(2,6-di*iso*propylphenyl)imidazolium chloride (IPr·HCl) according to literature procedures.[38] 1,3-bis(2,6-di*iso*propylphenyl)imidazolium chloride (IPr·HCl) was synthesized from 1,3-bis(2,6-di*iso*propylphenylimino) ethane according to literature procedures.[38] 1,2-Bis(2,6-di*iso*pro-pylphenylimino)ethane was synthesized from 1,3-bis(2,6-di*iso*propylphenyl)amine according to literature procedures.[39]

Fe(CO)$_5$ (Sigma Aldrich, trace metal basis), $Fe_2(CO)_9$, $Fe_3(CO)_{12}$ and Ph_3SiCl (all abcr GmbH) were bought and used as received.

^{1}H NMR spectra were recorded on Bruker spectrometers operating at 200, 300, 400 or 500 MHz; ^{13}C NMR spectra on Bruker spectrometers operating at 75.46, 100.61 or 125.758 MHz; ^{31}P NMR spectra were recorded on Bruker spectrometers operating at 101.28, 121.494, 161.97, 202.457 or 283.419 MHz. All ^{1}H and ^{13}C NMR chemical shifts are reported relative to $SiMe_4$ using the ^{1}H (residual) and ^{13}C chemical shifts of the solvent as a secondary standard (C_6D_6: δ 7.16 for ^{1}H, δ 128.06 for ^{13}C; CD_2Cl_2: δ 5.32 for ^{1}H, δ 53.50 for ^{13}C). ^{31}P chemical shifts are reported relative to an 85% H_3PO_4 solution in H_2O. Peak widths at half heights (in Hz) are given for broad signals. Data are reported as following: Chemical shift (δ) in ppm, multiplicity (s: singlet, d: doublet, dd:

 ©AUTHOR(S)

doublet of doublets, dt: doublet of triplets, t: triplet, td: triplet of doublets, q: quartet, qui: quintet, m: multiplet), coupling constants *J* (Hz) and integration.

Infrared spectra were collected on a Bruker-Alpha FT-IR-spectrometer. The absorption bands are labeled as following: strong (s 70-100%), middle (m 40-70%) and weak (w 10-40%).

Single crystals suitable for X-ray diffraction were protected with polyisobutylene oil under argon and measured on the Bruker D8-Venture diffractometer or a Bruker Apex 2 diffractometer using molybdenum irradiation.

Elemental analyses were performed at the Mikrolabor of ETH Zürich.

Scaled synthesis of 1,3-Bis(2,2'',4,4'',6,6''-hexamethyl-[1,1':3',1''-terphenyl]-2'-yl)-1,3,2l2,4l2-diazadiphosphetyl (1).

$[P(\mu\text{-N-TerCl})]_2$ was synthesized according to a modified literature procedure.[17]

Mg turnings can be activated by stirring under argon atmosphere for several days using a glass-covered magnetic-stirring bar. $[P(\mu\text{-N-TerCl})]_2$ (6.43 g, 8.16 mmol) and Mg turnings (2.87 g, 118 mmol) were combined in a Schlenk flask. *Attention: It is paramount to ensure that no grease finds its way into the reaction vessel.* THF (60 mL) was added, and the reaction mixture was stirred at ambient temperature. The colourless mixture gradually turned dark orange. The progress of the reaction was monitored by ^{31}P NMR spectroscopy, as over-reduction occurred quickly. When the reaction was completed, the reaction mixture was filtered over a stick frit in the glovebox, the solvent was removed *in vacuo* (1×10^{-3} mbar), and the solid residue was dried at 50 °C (water bath) for 30 minutes. Benzene (80 ml) was added, and the insoluble material was separated by filtration. If necessary, the cloudy filtrate was filtered a second time over a celite-packed frit. The intensive orange filtrate was concentrated to incipient crystallization. After crystallization overnight at ambient temperature, orange crystals of the product were obtained. The supernatant was removed by syringe and the isolated crystals were dried *in vacuo* (1×10^{-3} mbar) for 30 minutes at 50 °C (water bath). Afterwards the supernatant was concentrated, resulting in a second crop of orange crystals, which were treated in the same manner. Yield of first and second crop: 3.64 g (5.08 mmol, 62%).

^{1}H NMR (298 K, C_6D_6, 300.13 MHz): δ 2.04 (s, 24H, *o*-CH_3), 2.28 (s, 12H, *m*-CH_3), 6.73 (s, 8H, Mes *m*-C*H*), 6.73 (s, 4H, Mes *m*-C*H*), 6.89 (m, 2H, *m*-C*H*), 7.16 (m, 1H, *p*-C*H*). **^{13}C{^{1}H} NMR** (298 K, C_6D_6, 62.89 MHz): δ 18.5 (t, *o*-*C*H$_3$, J(^{13}C,^{31}P) 2.3 Hz), 19.7 (s, *p*-*C*H$_3$), 122.6 (s, *C*H), 126.8 (s, *C*H), 128.3 (s, *C*H), 130.6 (t, *C*, J(^{13}C,^{31}P) 1.6 Hz), 133.9 (t, *C*, J(^{13}C,^{31}P) 3.2 Hz), 135.7 (s, *C*), 136.35 (t, *C*, J(^{13}C,^{31}P) 3.4 Hz), 137.2 (m, *C*, J(^{13}C,^{31}P) 2.3 Hz). **^{31}P{^{1}H} NMR** (298 K, C_6D_6, 121.5 MHz): δ 276.3 (s).

Synthesis of 2-(4-(1,3-Bis(2,6-diisopropylphenyl)-1,3-dihydro-2*H*-imidazol-2-ylidene)-1λ^2,3λ^2-diphosphetyl-2-ylidene)-1,3-bis(2-isopropylphenyl)-2,3-dihydro-1*H*-imidazole (2)

An improved synthesis for **2** is presented (original protocol[13]), utilizing a modified procedure from Li[19] for the intermediate.

NaOCP · 7 dioxane (27.45 g, 38.83 mmol), 1,3-bis(2,6-diisopropylphenyl)-1,3-dihydro-2H-imidazol-2-ylidene (IPr; 10.0 g, 38.83 mmol, 1 eq.) and triphenyl(chloro)silane (11.45 g, 38.83 mmol, 1 eq.) were weighed into a 300 ml, small-necked Schlenk tube equipped with a stir bar inside the glove box. 150 ml of toluene and 5 ml of THF were added. The mixture was stirred at 70 °C for 2 h. A dark red, cloudy mixture was obtained. Subsequently, all volatiles were removed *in vacuo*, while the flask was warmed with a water bath ($1\cdot10^{-3}$ mbar for 1 h). The remaining solid was suspended in 100 ml *n*-hexane. (It may be necessary to add a second stir bar at this point, as the solid tends to immobilize the stirrer.) The suspension is cooled to −78 °C. KC_8 (5.77 g, 42.71 mmol, 1.2 eq.) is weighed into a separate Schlenk tube in the glove box and equipped with a bent glass tube with two male connectors and a glass cap. The Schlenk is connected to the reaction vessel *via* the bent tube in an argon counterflow. KC_8 Is added to the cold suspension by carefully shaking the setup. The smaller

 ©AUTHOR(S)

vessel is removed, and the flask sealed with a stopcock. Afterwards, the reaction mixture is allowed to warm to room temperature. Stirring is continued.

After 16 h, a dark green mixture was obtained. It was transferred onto a G4 sintered frit, and packed with a generous pad of celite. The solution was collected. Volatiles were removed *in vacuo* via the tab on the receiver flask ($1\cdot10^{-3}$ mbar for 1 h, for a scheme of the setup see the SM). Afterwards, 150 ml of diethyl ether were added to the solid on top of the frit and filtered through. The stopcock on the frit was replaced with a reflux condenser, connected to a tap. The tab on the receiver flask was closed and the one on top of the reflux condenser opened. The flask was heated to 60 °C with an oil bath, so that the solvent evaporated, condensed in the reflux condenser, and extracted the solids on top of the frit (compare the scheme in the SM). The extraction was continued until the solution washing through the frit became almost colourless. (Towards the end, the solution went from green to lightly brown. At that point, the extraction was stopped.)

Subsequently, the receiver flask was disconnected from the extraction setup and sealed with a stopcock. Volatiles were removed *in vacuo* ($1\cdot10^{-3}$ mbar for 1 h). The remaining dark solid was suspended in 120 ml of acetonitrile and transferred onto another G4 sintered frit. Filtration gave a brown filtrate and a green solid. The solid was washed three times with 10 ml acetonitrile each. The receiver flask was then disconnected and the solid briefly dried *in vacuo* ($1\cdot10^{-3}$ mbar for 15 min).

Finally, a new receiver flask is connected to the frit. The solid is extracted with 100 ml of diethyl ether into the flask. Volatiles were removed *in vacuo*.

The product obtained *via* this route was of sufficient purity for follow-up reactions. Samples of very high purity may be obtained by recrystallization from hot *n*-hexane.

Yield: 6.0 g (6.989 mmol; 36%).

^{1}H NMR (C_6D_6, 500.1 MHz): δ [ppm] 1.19 (d, $^{3}J(^{1}H, ^{1}H)$ 6.6 Hz, 12 H, CH(CH_3)$_2$), 1.35 (d, $^{3}J(^{1}H, ^{1}H)$ 6.5 Hz, 12 H, CH(CH_3)$_2$), 2.99 (m, $^{3}J(^{1}H, ^{1}H)$ 6.7 Hz, 4 H, CH(CH$_3$)$_2$), 5.99 (s, 2H, NCH), 7.05 (d, $^{3}J(^{1}H, ^{1}H)$ 7.7 Hz, 4H, *meta*-C^{ar}H), 7.25 (t, $^{3}J(^{1}H, ^{1}H)$ 7.7 Hz, 2H, *para*-C^{ar}H). **^{13}C{^{1}H} NMR** (C_6D_6, 125.8 MHz): δ [ppm] 23.6 (s, 4C, CH(*C*H$_3$)$_2$), 25.0 (s, 4C, CH(*C*H$_3$)$_2$), 29.1 (s, 4C, *C*H(CH$_3$)$_2$), 118.3 (s, 4C, N*C*H), 124.3 (4C, *para*-*C*^{ar}), 129.7 (s, 8C, *meta*-*C*^{ar}), 131.0 (t, $^{1}J(^{13}C, ^{31}P)$ 41 Hz, 2 C, C*C*P), 134.5 (s, 4C, *ipso*-*C*^{ar}), 147.7 (s, 8C, *ortho*-*C*^{ar}), 152.1 (t, $^{2}J(^{13}C, ^{31}P)$ 14 Hz, 2 C, N*C*N). **^{31}P{^{1}H} NMR** (C_6D_6, 202.5 MHz): δ [ppm] 196.3 (s, 2P, C*P*C).

Synthesis of (1,3-Bis(2,2'',4,4'',6,6''-hexamethyl-[1,1':3',1''-terphenyl]-2'-yl)-1,3,2,4λ^2-2-diazadiphosphetidin-2-yl)tetracarbonyliron (5)

A round bottomed Schlenk flask was equipped with a stirrer bar and charged with 162 mg (0.226 mmol) [P(μ-NTer)]$_2$ (Ter: 2,6-bis(2,4,6-trimethylphenyl)-phenyl)), 82 mg (0.226 mmol) Fe_2CO_9 and 5 ml toluene. After stirring the mixture at room temperature for 20 h, volatiles were removed *in vacuo* ($1\cdot10^{-3}$ mbar for 1 h). The crude product was recrystallized from *n*-hexane by cooling a saturated solution from 60 °C to −20 °C, yielding a black, microcrystalline product.

Yield: 0.124 g (0.0140 mmol; 62%).

Melting point: 191 °C (dec.). **CHN** for $C_{52}H_{50}FeN_2O_4P_2$ (884.775 g·mol^{-1}) found (calc.): C 71.95 (70.59), H 5.81 (5.70), N 3.49 (3.17). **^{1}H NMR** (CD_2Cl_2, 500.1 MHz): δ [ppm] 1.94 (s, 12H, Mes-*ortho*-CH_3), 1.97 (s, 12H, Mes-*ortho*-CH_3), 2.42 (s, 12H, Mes-*para*-CH_3), 6.80 (s, 4H, Mes-*meta*-*H*), 6.82 (s, 4H, Mes-*meta*-*H*), 6.87 (d, $^{3}J(^{1}H, ^{1}H)$ 7.5 Hz, 4H, *meta*-CH_3), 7.13 (t, $^{3}J(^{1}H, ^{1}H)$ 7.5 Hz, 2H, *para*-CH_3). **^{13}C{^{1}H} NMR** (CD_2Cl_2, 125.8 MHz) δ [ppm] 20.9 (s, 4C, *para*-*C*H$_3$), 21.5 (s, 4C, *ortho*-*C*H$_3$), 21.6 (s, 4C, *ortho*-*C*H$_3$), 125.5 (s, 2C, *para*-*C*H), 129.2 (s, 4C, Mes-*meta*-*C*H), 129.7 (s, 4C, Mes-*meta*-*C*H), 131.9 (s, 4C, *meta*-*C*H), 132.8 (s, 4C, *ipso*-*C*), 135.7 (s, 4C, *ipso*-*C*), 137.2 (s, 4C, *ipso*-*C*), 137.6 (s, 2C, N*C*), 138.3 (s, 4C, *ipso*-*C*), 138.5 (s, 4C, *ipso*-*C*), 217.4 (s, 4C, *C*O). **^{31}P{^{1}H} NMR** (CD_2Cl_2, 202.5 MHz): δ [ppm] 275.3 (d, $^{2}J(^{31}P, ^{31}P)$ 174 Hz, 1P, N(Fe)*P*N), 357.1 (d, $^{2}J(^{31}P, ^{31}P)$ 174 Hz, 1P, N*P*N). **IR** (transmission, sat. *n*-hexane solution, 25 °C, 64 Scans): $\tilde{\nu}$ [cm^{-1}]: 2034 (m), 1967 (m), 1949 (s). **IR** (ATR, 25 °C,

 ©AUTHOR(S)

64 Scans): ṽ [cm^{-1}]: 2959 (w), 2908 (w), 2115 (w), 2025 (s), 1935 (s), 1610 (w), 1430 (w), 1404 (m), 1373 (w), 1336 (w), 1260 (m), 1235 (w), 1219 (s), 1160 (w), 1084 (w), 1015 (m), 947 (w), 930 (m), 912 (w), 872 (w), 842 (m), 795 (s), 761 (m), 745 (w), 734 (w), 686 (s), 631 (m), 618 (w), 607 (s), 572 (w), 548 (w), 521 (w), 509 (w), 474 (w), 456 (w), 428 (m).

Synthesis of (2-(1,3-Bbis(2,6-diisopropylphenyl)-1,3-dihydro-2*H*-imidazol-2-ylidene)-4-(1,3-bis(2-isopropyl-phenyl)-1,3-dihydro-2*H*-imidazol-2-ylidene)-1,3λ^2-diphosphetan-1-yl)tetracarbonylliron (6)

A Schlenk flask was equipped with a stirrer bar and charged with 400 mg (0.463 mmol) $(IPrCP)_2$, and 10 ml toluene. While being stirred at room temperature, $Fe(CO)_5$ (0.08 ml, 0.597 mmol, 1.3 eq) was added *via* microsyringe. The solution turned first brown, then intensely purple. Moderate gas development was observed at the pressure release valve of the Schlenk line. After stirring the mixture at room temperature for 20 h, volatiles were removed *in vacuo* ($1\cdot10^{-3}$ mbar for 1 h). The crude product was washed with hot *n*-hexane and dried *in vacuo* at ambient temperature ($1\cdot10^{-3}$ mbar for 3 h), yielding a black solid.

Yield: 276 mg (0.0278 mmol; 60%).

Melting point: 305 °C. **CHN** for $C_{60}H_{72}FeN_4O_4P_2$ (1031.053 g·mol^{-1}) found (calc.): C 70.12 (69.90), H 6.57 (7.04), N 5.42 (5.43). **^{1}H NMR** (C_6D_6, 500.1 MHz): δ [ppm] 0.96 (d, $^3J(^1H, ^1H)$ 6.9 Hz, 6 H, $CH(CH_3)_2$), 0.99 (d, $^3J(^1H, ^1H)$ 6.7 Hz, 6 H, $CH(CH_3)_2$), 1.06 (d, $^3J(^1H, ^1H)$ 7.1 Hz, 6 H, $CH(CH_3)_2$), 1.08 (d, $^3J(^1H, ^1H)$ 7.1 Hz, 6 H, $CH(CH_3)_2$), 1.22 (d, $^3J(^1H, ^1H)$ 6.7 Hz, 6 H, $CH(CH_3)_2$), 1.29 (d, $^3J(^1H, ^1H)$ 6.6 Hz, 6 H, $CH(CH_3)_2$), 1.37 (d, $^3J(^1H, ^1H)$ 6.5 Hz, 6 H, $CH(CH_3)_2$), 1.81 (d, $^3J(^1H, ^1H)$ 6.5 Hz, 6 H, $CH(CH_3)_2$), 2.65 (m, $^3J(^1H, ^1H)$ 6.8 Hz, 2 H, $CH(CH_3)_2$), 3.07 (m, $^3J(^1H, ^1H)$ 6.7 Hz, 2 H, $CH(CH_3)_2$), 3.33 (m, $^3J(^1H, ^1H)$ 6.7 Hz, 2 H, $CH(CH_3)_2$), 3.60 (m, $^3J(^1H, ^1H)$ 6.6 Hz, 2 H, $CH(CH_3)_2$), 6.04 (d, $^5J(^1H, ^{31}P)$ 1.6 Hz, 2 H, NC*H*), 6.25 (d, $^5J(^1H, ^{31}P)$ 1.4 Hz, 2 H, NC*H*), 6.92 (d, $^3J(^1H, ^1H)$ 7.7 Hz, 2H, *meta*-$C^{ar}H$), 7.01 (d, $^3J(^1H, ^1H)$ 7.6 Hz, 2H, *meta*-$C^{ar}H$), 7.1 (2H, *meta*-$C^{ar}H$, overlap with solvent signal), 7.23 (d, $^3J(^1H, ^1H)$ 7.7 Hz, 2H, *meta*-$C^{ar}H$), 7.1 (2H, *para*-$C^{ar}H$, overlap with solvent signal), 7.31 (t, $^3J(^1H, ^1H)$ 7.7 Hz, 2H, *para*-$C^{ar}H$). **^{13}C{^{1}H} NMR** (C_6D_6, 125.8 MHz): δ [ppm] 22.8 (s, 1C, $CH(CH_3)_2$), 23.0 (s, 1C, $CH(CH_3)_2$), 23.2 (s, 1C, $CH(CH_3)_2$), 23.9 (s, 1C, $CH(CH_3)_2$), 25.5 (s, 2C, $CH(CH_3)_2$), 25.5 (s, 1C, $CH(CH_3)_2$), 27.9 (s, 1C, $CH(CH_3)_2$), 28.3 (s, 1C, $CH(CH_3)_2$), 28.5 (s, 1C, $CH(CH_3)_2$), 28.7 (s, 1C, $CH(CH_3)_2$), 29.3 (s, 1C, $CH(CH_3)_2$), 119.9 (s, 2C, NCH), 121.4 (s, 2C, NCH), 124.3 (1C, *para*-C^{ar}), 124.7 (1C, *para*-C^{ar}), 125.4 (1C, *para*-C^{ar}), 125.7 (1C, *para*-C^{ar}),130.6 (s, 4C, *meta*-C^{ar}), 130.9 (s, 4C, *meta*-C^{ar}), 133.4 (s, 2C, *ipso*-C^{ar}), 134.3 (s, 2C, *ipso*-C^{ar}), 144.7 (t, $^1J(^{13}C, ^{31}P)$ 38 Hz, 2 C, CCP), 145.1 (s, 2C, *ortho*-C^{ar}), 147.2 (s, 2C, *ortho*-C^{ar}), 147.2 (s, 2C, *ortho*-C^{ar}), 147.6 (s, 2C, *ortho*-C^{ar}), 151.6 (t, $^2J(^{13}C, ^{31}P)$ 11 Hz, 2 C, NCN), 214.8 (s, 2C, CO, $\nu_{1/2}$ 50 Hz), 221.4 (s, 2C, CO, $\nu_{1/2}$ 130 Hz). **^{31}P{^{1}H} NMR** (C_6D_6, 202.5 MHz): δ [ppm] 79.8 (d, $^2J(^{31}P, ^{31}P)$ 119 Hz, 1P, CP(Fe)C), 325.7 (d, $^2J(^{31}P, ^{31}P)$ 119 Hz, 1P, CPC). **IR** (transmission, sat. *n*-hexane solution, 25 °C, 64 scans): ṽ [cm^{-1}]: 2001 (s), 1928 (w), 1900 (m), 1886 (s). **IR** (ATR, 25 °C, 64 scans): ṽ [cm^{-1}]: 2962 (w), 2927 (w), 2866 (w), 1998 (s), 1911 (sh), 1895 (sh), 1882 (s), 1456 (w), 1426 (s), 1382 (w), 1360 (w), 1332 (s), 1302 (w), 1261 (m), 1216 (m), 1205 (w), 1193 (w), 1147 (w), 1126 (w), 1080 (w), 1058 (w), 1046 (m), 1015 (m), 933 (w), 910 (m), 861 (w), 798 (s), 751 (m), 724 (w), 715 (w), 695 (m), 686 (w), 617 (s), 545 (w), 529 (w), 506 (w), 478 (w), 462 (w), 437 (w), 412 (w).

Acknowledgements

This work was supported by the Swiss National Science Foundation (SNF; grant 2-77199-18) and the ETH Zürich (grant 0-20406-18). PC gratefully acknowledges funding by the Deutsche Forschungsgemeinschaft (DFG, grant 438203135). We thank Dr. M. Wöhrle for valuable help with the X-ray diffraction measurements and Dr. R. Vérel for valuable help with acquisition and interpretation of NMR data.

 ©AUTHOR(S)

We gratefully acknowledge financial support by the Deutsche Forschungsgemeinschaft (DFG; SCHU 1170/12-2).

Supplementary Material

A scheme of the apparatus for the synthesis of **2**, detailed spectra, calculations and crystallographic data are available in the Supplementary Material associated with this paper.

References

1. Li, Z.; Hou,Y.; Li, Y.; Hinz, A.; Chen, X. *Chem. - Eur. J.* **2018**, *24*, 4849-4855. https://doi.org/10.1002/chem.201705403.
2. Breher, F.; *Coord. Chem. Rev.* **2007**, *251*, 1007-1043. https://doi.org/10.1016/j.ccr.2006.09.007
3. Schulz, A. *Dalton Trans.* **2018**, *47*, 12827-12837. https://doi.org/10.1039/c8dt03038c.
4. Bresien, J.; Eickhoff, L.; Schulz, A.; Zander, E. *Biradicals in main group chemistry: Synthesis, electronic structure, and application in small-molecule activation*, Elsevier, 2021. https://doi.org/10.1016/B978-0-12-823144-9.00029–7
5. Niecke, E.; Fuchs, A.; Baumeister, F.; Nieger, M.; Schoeller, W. W. *Angew. Chem. Int. Ed.* **1995**, *34*, 555-557 https://doi.org/10.1002/anie.199505551
6. Schoeller, W. W. *Eur. J. Inorg. Chem.* **2019**, *2019*, 1495-1506. https://doi.org/10.1002/ejic.201801218
7. Hinz, A.; Schulz, A.; Villinger, A. *Chem. Commun.* **2016**, *52*, 6328-6331. https://doi.org/10.1039/c6cc01935h.
8. Scharnhölz, M. T.; Coburger, P.; Gravogl, L.; Klose, D.; Gamboa-Carballo, J. J.; Le Corre, G.; Bosken, J.; Schweinzer, C.; Thony, D.; Li, Z.; Meyer, K.; Grützmacher, H. *Angew. Chem. Int. Ed.* **2022**, *61*, e202205371. https://doi.org/10.1002/anie.202205371
9. Steffenfauseweh, H.; Vishnevskiy, Y. V.; Neumann, B.; Stammler, H.-G.; Andrada, D. M.; Ghadwal, R. *Angew. Chem. Int. Ed.* **2022**, *n/a.* https://doi.org/10.1002/anie.202207415
10. Scheschkewitz, D.; Amii, H.; Gornitzka, H.; Schoeller, W. W.; Bourissou, D.; Bertrand, G. *Science* **2002**, *295*, 1880-1881. https://doi.org/10.1126/science.1068167
11. Cui, C.; Brynda, M.; Olmstead, M. M.; Power, P. P. *J. Am. Chem. Soc.* **2004**, *126*, 6510-6511. https://doi.org/10.1021/ja0492182
12. Beweries, T.; Kuzora, R.; Rosenthal, U.; Schulz, A.; Villinger, A. *Angew. Chem. Int. Ed.* **2011**, *50*, 8974-8978. https://doi.org/10.1002/anie.201103742
13. Li, Z.; Chen, X.; Andrada, D. M.; Frenking, G.; Benko, Z.; Li, Y.; Harmer, J. R.; Su, C. Y.; Grützmacher, H. *Angew. Chem. Int. Ed.* **2017**, *56*, 5744-5749. https://doi.org/10.1002/anie.201612247

 ©**AUTHOR(S)**

14. Hinz, A.; Kuzora, R.; Rosenthal, U.; Schulz, A.; Villinger, A. *Chem. - Eur. J.* **2014**, *20*, 14659-14673. https://doi.org/10.1002/chem.201403964
15. Chen, X.; Liu, L. L.; Liu, S.; Grützmacher, H.; Li, Z. *Angew. Chem. Int. Ed.* **2020**, *59*, 23830-23835. https://doi.org/10.1002/anie.202011677
16. Li, Z.; Chen, X.; Liu, L. L.; Scharnhölz, M. T.; Grützmacher, H. *Angew. Chem. Int. Ed.* **2020**, *59*, 4288-4293. https://doi.org/10.1002/anie.201914015
17. Beer, H.; Blasing, K.; Bresien, J.; Chojetzki, L.; Schulz, A.; Stoer, P.; Villinger, A. *Dalton Trans.* **2020**, *49*, 13655-13662. https://doi.org/10.1039/d0dt03251d
18. Rottschafer, D.; Neumann, B.; Stammler, H. G.; Ghadwal, R. S. *Chem. - Eur. J.* **2017**, *23*, 9044-9047. https://doi.org/10.1002/chem.201702433
19. Li, Z.; Chen, X.; Li, Y.; Su, C. Y.; Grutzmacher, H. *Chem. Commun.* **2016**, *52*, 11343-11346. https://doi.org/10.1039/c6cc05916c
20. Addison, A. W.; Rao, T. N.; Reedijk, J.; van Rijn, J.; Verschoor, G. C. *Dal*1349-1356. https://doi.org/10.1039/dt9840001349
21. Tiana, D.; Francisco, E.; Blanco, M. A.; Macchi, P.; Sironi, A.; Martín Pendás, A. *J. Chem. Theory Comput.* **2010**, *6*, 1064-1074. https://doi.org/10.1021/ct9006629
22. Palomo-Molina, J.; Garcia-Baez, E. V.; Contreras, R.; Pineda-Urbina, K.; Ramos-Organillo, A. *Acta Crystallogr C Struct Chem* **2015**, *71*, 788-792. https://doi.org/10.1107/S2053229615014503
23. Bistoni, G.; Rampino, S.; Scafuri, N.; Ciancaleoni, G.; Zuccaccia, D.; Belpassi, L.; Tarantelli, F. *Chem. Sci.* **2016**, *7*, 1174-1184. https://doi.org/10.1039/c5sc02971f
24. Rossi, A. R.; Hoffmann, R. *Inorganic Chemistry* **1975**, *14*, 365-374. https://doi.org/10.1021/ic50144a032
25. Berry, R. S. *J. Chem. Phys.* **1960**, *32*, 933-938. https://doi.org/10.1063/1.1730820
26. King, R. B.; Korenowski, T. F. *Inorg. Chem.* **1971**, *10*, 1188-1195. https://doi.org/10.1021/ic50100a018
27. Schumann, H.; Rösch, L.; Kroth, H.-J.; Neumann, H.; Neudert, B. *Chem. Ber.* **1975**, *108*, 2487-2499. https://doi.org/10.1002/cber.19751080802
28. Barnard, T. S.; Mason, M. R. *Inorg. Chem.* **2001**, *40*, 5001-5009. https://doi.org/10.1021/ic001372b
29. Schubert, E. H.; Sheline, R. K. *Inorg. Chem.* **1966**, *5*, 1071-1074. https://doi.org/10.1021/ic50040a024
30. Fischer, E. O.; Louis, E.; Bathelt, W.; Müller, J. *Chem. Ber.* **1969**, *102*, 2547-2556. https://doi.org/10.1002/cber.19691020808
31. Warratz, S.; Postigo, L.; Royo, B. *Organometallics* **2013**, *32*, 893-897. https://doi.org/10.1021/om3012085
32. Neese, F. *WIREs Computational Molecular Science* **2017**, *8*. https://doi.org/10.1002/wcms.1327
33. Neese, F. W. F.; Becker, U.; Riplinger, C. *J. Chem. Phys.* **2020**, *152*, 224108. https://doi.org/10.1063/5.0004608

 ©**AUTHOR(S)**

34. Tao, J.; Perdew, J. P.; Staroverov, V. N.; Scuseria, G. E. *Phys. Rev. Lett.* **2003**. https://doi.org/10.1103/PhysRevLett.91.146401, 146401
35. Grimme, S.; Antony, J.; Ehrlich, S.; Krieg, H. *J. Chem. Phys.* **2010**, *132*, 154104. https://doi.org/10.1063/1.3382344
36. Grimme, S.; Ehrlich, S.; Goerigk, L. *J. Comput. Chem.* **2011**, *32*, 1456-1465. https://doi.org/10.1002/jcc.21759
37. Weigend, F.; Ahlrichs, R. *Phys. Chem. Chem. Phys.* **2005**, *7*, 3297-3305. https://doi.org/10.1039/b508541a
38. Arduengo, A. J.; Krafczyk, R.; Schmutzler, R.; Craig, H. A.; Goerlich, J. R.; Marshall, W. J.; Unverzagt, M. *Tetrahedron* **1999**, *55*, 14523-14534. https://doi.org/10.1016/s0040-4020(99)00927-8
39. Wang, Y.; Yang, X. L.; Zhang, C. Y.; Yu, J. Q.; Liu, J. H.; Xia, C. G. *Adv Synth Catal* **2014**, *356*, 2539-2546. https://doi.org/10.1002/adsc.201400040.

This paper is an open access article distributed under the terms of the Creative Commons Attribution (CC BY) license (http://creativecommons.org/licenses/by/4.0/)